Unmanned aerial vehicle swarm control using potential functions and sliding mode control

K Han, J Lee, and **Y Kim***
School of Mechanical and Aerospace Engineering, Institute of Advanced Aerospace Technology, Seoul National University, Seoul, Republic of Korea

The manuscript was received on 20 March 2008 and was accepted after revision for publication on 4 June 2008.

DOI: 10.1243/09544100JAERO352

Abstract: This paper deals with a behaviour-based decentralized control strategy for unmanned aerial vehicle (UAV) swarming by using artificial potential functions and sliding mode control technique. Individual interactions for swarming behaviour are modelled using the artificial potential functions. For tracking the reference trajectory of the swarming of UAVs, a swarming centre is considered as the object of control. The sliding-mode control technique is adopted to make the proposed swarm control strategy robust with respect to the system uncertainties and varying mission environment. Collision avoidance against obstacles and pop-up threats is also considered. Numerical simulations are performed to verify the performance of the proposed controller.

Keywords: unmanned aerial vehicle swarming, potential function, sliding mode control, obstacle avoidance

1 INTRODUCTION

The unmanned aerial vehicles (UAVs) play an important role in various fields that are rapidly evolving with the demands for fulfilling multi-purpose mission objectives. Consequently, there have been many studies on the formation flight control systems to make multiple UAVs perform the missions cooperatively and autonomously accomplish the objectives. The behaviour of such a system is similar to aggregation behaviour in nature, for example, the highly coordinated movements of flock of birds or school of fishes. These examples have motivated the researchers to apply the concept of 'swarming' to the flying formation of multiple UAVs.

In general, formation flight control is divided by the roles of each aircraft, for example, leader–follower and virtual structure. Leader–follower approach is the most popular way of the formation flight in which the leader flies along the path and the other follows the leader while keeping a certain distance. However, in case that the leader has a problem, the formation can be easily broken down. Also there exist error propagation and time delay in the communication. Virtual structure approach was developed to overcome the weak points in the leader–follower method; however, it has difficulties in the mathematical approach and requires a lot of calculation. In recent studies, swarm technology has been suggested as a possible solution to automatically control and coordinate multiple UAVs. A swarm consists of a large number of individuals in parallel so that it is able to perform a mission as a group as long as they keep a certain distance from each other. Formation flight control is less efficient when compared with swarm control because the formation flight control has to keep the formation under any occasion, and another technique has to be added for a collision avoidance or formation reconfiguration. Also, as more agents involve in, the formations become more complicated. Swarm has an advantage of dealing with varying environments and can be used in the field that requires instinct behaviour such as collision avoidance and search and rescue.

As UAVs are required to be operated in groups, collision avoidance becomes one of the important issues

**Corresponding author: School of Mechanical and Aerospace Engineering, Institute of Advanced Aerospace Technology, Seoul National University, Shinlim-Dong, Gwanak-Ku, Seoul 151-742, Republic of Korea. email: ydkim@snu.ac.kr*

in the UAV swarm control system. The centralized control scheme has been studied much for UAV formation control, but it is not suitable for swarm. Therefore, it is necessary for a swarm controller to have a strategy that each agent reaches the destination without collision, by recognizing the locations of threats and obstacles as well as the other agents of the group.

There have been some previous works to emulate the swarm behaviours in nature [**1**]. One method is to use optimization theory, however, this method has problems that it requires much computation time and adaptation to the real time operation is difficult. To overcome these disadvantages, the control strategy of the multi-agent system based on the artificial potential functions and sliding-mode control technique was introduced [**2**, **3**]. In references [**4**], [**5**], and [**6**], the path planning and obstacle avoidance of the robots was proposed based on the artificial potential function. Potential function and sliding mode control were also applied to the problem of tracking the moving target [**7**, **8**].

In this paper, the swarm modelling is modified using potential field method and the concept of swarm geometry centre (SGC) control. Controlling SGC does not require the path generation for each aircraft, and is only used for the imaginary point in swarm geometry so that it is much easier to control a swarm and to track a trajectory. Also, this paper suggests a modified collision avoidance method preventing local minima without generating new path when the UAVs meet the pop-up threats. And Voronoi diagram and A* algorithm [**9**, **10**] are used to generate the reference trajectory for SGC where obstacles exist near the path. To avoid collision with obstacles, all the obstacles are included in the potential function.

In this paper, the potential function is adopted to model the swarm procedure [**11**], and the sliding mode control is applied for UAV swarm to have the robustness of the controller with respect to various system uncertainties. The swarm strategy is modified such that the swarm formation is maintained while the UAVs are following the reference trajectory by controlling the SGC. In references [**12**] and [**13**], instead of following the pre-assigned member, each agent can keep its position with respect to the imaginary point, i.e. the centre of the swarm geometry. Under the assumption that each agent autonomously keeps the prescribed formation, the SGC control allows the swarm track, the reference trajectory, well. Collision avoidance method against the obstacles is also considered. With the advantage of potential function method, the collision avoidance can be easily treated. The pop-up threat avoidance algorithm is also introduced by modifying the shape of obstacle. Numerical simulations are performed to validate the performance of the proposed strategy.

2 SWARM MODELLING AND SGC CONTROL

The behaviour of every agent in the swarm can be modelled based on several simple rules, where the agents interact with each other. Each individual does not behave in compliance to commands from a leader, but autonomously interact with other agents and environment. Such behaviour pattern can be classified as a decentralized control scheme [**14**]. Reynolds [**15**] created a 'Boid' model or birdoid (bird-like) model to simulate the decentralized swarm behaviour. In this model, each agent follows the three basic behaviour rules: avoidance rule, velocity matching rule, and flock centre rule.

Consider a swarm composed of N UAVs. Flying towards the destination without conflict, while keeping certain distance between the agents, is mandatory for swarm control. Based on the potential field method, the UAV flies under the influence of an artificial field of forces that are produced by other UAVs around it. In order to emulate the swarm behaviours, the potential function represented by the relative distances between agents is considered

$$J(x) = \sum_{i=1}^{N-1} \sum_{j=i+1}^{N} J_{ij}\|x^i - x^j\| \tag{1}$$

where $\boldsymbol{x}^i \in R^n$ is a position vector of each agent. The path of each agent is then generated by following the negative gradient of the potential as [**16**]

$$\dot{x}^i = -\nabla_{x^i} J(x), \quad i = 1, \ldots, N \tag{2}$$

Several assumptions are required for swarm aggregation avoiding collision in the specified region [**3**]

Assumption 1

The potential function is symmetric to the position vector of the individuals [**3**], that is

$$\nabla_{x^i} J_{ij}\|x^i - x^j\| = -\nabla_{x^j} J_{ij}\|x^i - x^j\| \tag{3}$$

Assumption 2

There exists gradient function of potential function, and it is composed of attractive potential function (J_a^{ij}) and repulsive potential function (J_r^{ij}) [**3**] as

$$\begin{aligned}\nabla_{x^i} J_{ij}\|x^i - x^j\| &= \nabla_{x^i} J_a^{ij}\|x^i - x^j\| + \nabla_{x^i} J_r^{ij}\|x^i - x^j\| \\ &= (x^i - x^j) g_{\mathrm{ar}}^{ij}\|x^i - x^j\|\end{aligned} \tag{4}$$

where $x^i - x^j$ is the direction vector between agents and g_{ar}^{ij} the scalar potential function that represents the summation of repulsive and attractive potential.

Assumption 3

There exist a steady distance δ_{ij} which satisfies the following conditions [3]

$$\begin{aligned} &g_{\text{ar}}^{ij}\|x^i - x^j\| = 0, \quad \|x^i - x^j\| = \delta_{ij} \\ &g_{\text{ar}}^{ij}\|x^i - x^j\| > 0, \quad \|x^i - x^j\| > \delta_{ij} \\ &g_{\text{ar}}^{ij}\|x^i - x^j\| < 0, \quad \|x^i - x^j\| < \delta_{ij} \end{aligned} \tag{5}$$

To the potential function satisfying the above assumptions and the following theorems can be derived in case of zero initial velocity [3].

Theorem 1

The swarm centre $x_G = 1/N \sum_{i=1}^{N} x^i$ is stationary all the time [3].

Theorem 2

Convergence to invariant set as $t \to \infty$ for any initial condition $x(0) \in \mathbb{R}^{nN}$ occurs [3].

Proofs for these theorems are given in reference [3]. These theorems imply that the potential function satisfying the assumptions converges within a certain distance from the swarm centre without a collision. Accordingly, this follows the avoidance rule and the flock centre rule. In this study, the following potential function is adopted [3]

$$J_{ij}(x) = \frac{c_1}{2}\|x^i - x^j\|^2 + \frac{c_2 c_3}{2}\exp\left(-\frac{\|x^i - x^j\|^2}{c_3}\right) \tag{6}$$

This potential function satisfies all the above-said assumptions. The first term is the attractive potential function, and second the repulsive potential function. The equilibrium distance between the agents is obtained by

$$\delta_{ij} = \sqrt{c_3(\log c_2 - \log c_1)} \tag{7}$$

Note that the geometry shape and the size of the swarm depend on c_i's that represent the magnitudes of attractive and repulsive potential functions and influence a range of repulsive potential. In order to follow the reference trajectory while keeping the formation shape, a formation geometry centre (FGC) control strategy, which is a sort of decentralized formation control, is applied. There is no need for considering the path of multiple UAVs in case of FGC method. Instead, any path planning and guidance algorithm for a single UAV is easily applicable to multiple UAVs by combining two controllers: (a) for keeping the formation shape, (b) for tracking the reference trajectory. This FGC control strategy has an additional advantage that it can easily deal with various dynamic environments such as collision avoidance, which will be discussed in more detail in later sections.

SGC is defined as

$$x_{\text{SGC}} = \frac{1}{N}\sum_{i=1}^{N} x^i \tag{8}$$

To control the SGC, it is considered as a virtual UAV and the guidance law is applied for tracking the reference trajectory. Velocity command ($\dot{x}_{\text{SGC}_{\text{command}}}$) and acceleration command ($\ddot{x}_{\text{SGC}_{\text{command}}}$) can be designed to follow the desired reference trajectory using various guidance laws. Then

$$\dot{x}^i = \dot{x}^i_{\text{swarm}} + \dot{x}^i_{\text{reference}} = -\nabla_{x^i} J(x) + \dot{x}_{\text{SGC}_{\text{command}}} \tag{9}$$

As mentioned in Theorem 2, the velocity of the agent converges to the invariant set as $t \to \infty$, and finally the velocities of all agents matches to that of SGC. Thus, the potential function and the SGC strategy proposed in this study satisfy all the three behaviour rules of the 'Boid' model.

3 SLIDING MODE CONTROL

3.1 UAV model

Consider the following two-dimensional point mass model

$$\begin{aligned} &\dot{x} = V\cos\psi; \quad \dot{y} = V\sin\psi; \quad \dot{V} = u_1 - f_1; \\ &\dot{\psi} = \frac{u_2 - f_2}{V} \end{aligned} \tag{10}$$

where f_i is the system uncertainty, and is assumed that it is bounded as

$$|f_i| \leqslant \bar{f}_i \tag{11}$$

Equation (10) can be rewritten as

$$\begin{bmatrix} \ddot{x} \\ \ddot{y} \end{bmatrix} = \begin{bmatrix} \cos\psi & -\sin\psi \\ \sin\psi & \cos\psi \end{bmatrix} \left\{ \begin{bmatrix} u_1 \\ u_2 \end{bmatrix} - \begin{bmatrix} f_1 \\ f_2 \end{bmatrix} \right\} \tag{12}$$

To simplify equation (12), the transformation matrix $\mathbf{T}(\psi)$ is defined as

$$\mathbf{T}(\psi) \equiv \begin{bmatrix} \cos\psi & -\sin\psi \\ \sin\psi & \cos\psi \end{bmatrix} \tag{13}$$

Substituting equation (13) in equation (12) yields

$$\ddot{x}^i = \mathbf{T}(\psi)(u^i - f^i) \tag{14}$$

where $x^i = [x \quad y]^{\mathrm{T}}$, $u^i = [u_1 \quad u_2]^{\mathrm{T}}$, $f^i = [f_1 \quad f_2]$, and superscript i denotes the ith UAV.

3.2 Sliding mode controller

In this study, the sliding mode controller is adopted to make the proposed swarm control strategy robust with respect to the system uncertainties and the varying mission environments. To control the velocity of each agent in equation (9), the sliding surface is defined as follows

$$s^i = \dot{x}^i + \nabla_{x^i} J(x) - \dot{x}_{\mathrm{SGC}_{\mathrm{command}}} = 0 \tag{15}$$

To design a sliding mode controller, consider a Lyapunov candidate function as

$$V = \frac{1}{2} s^{i\mathrm{T}} s^i \tag{16}$$

Differentiating equation (16) with respect to time, and by using equation (14)

$$\begin{aligned}\dot{V}^i &= s^{i\mathrm{T}} \dot{s}^i = s^{i\mathrm{T}} \left\{ \ddot{x} + \frac{\mathrm{d}}{\mathrm{d}t}[\nabla_{x^i} J(x)] - \ddot{x}_{\mathrm{SGC}_{\mathrm{command}}} \right\} \\ &= s^{i\mathrm{T}} \left\{ T_i(\psi)(u^i - f_i) + \frac{\mathrm{d}}{\mathrm{d}t}[\nabla_{x^i} J(x)] - \ddot{x}_{\mathrm{SGC}_{\mathrm{command}}} \right\}\end{aligned} \tag{17}$$

The above equation requires the differentiation of potential function. Applying the chain rule to the potential function, and using the sliding surface defined in equation (15)

$$\begin{aligned}\left\| \frac{\mathrm{d}}{\mathrm{d}t}[\nabla_{x^i} J(x)] \right\| &= \left\| \sum_{j=1}^{N} \{\nabla_{x^j}[\nabla_{x^i} J(x)] \dot{x}^j\} \right\| \\ &= \left\| \sum_{j=1}^{N} \{[\nabla_{x^j}[\nabla_{x^i} J(x)]]\} \{[s^j - \nabla_{x^j} J(x) + \dot{x}_{\mathrm{SGC}_{\mathrm{command}}}]\} \right\|\end{aligned} \tag{18}$$

Note that the potential function used in this study, equation (6), is in C^2, and it satisfies the following conditions

$$\|\nabla_{x^i} J(x)\| \leqslant \alpha(x); \quad \|\nabla_{x^j}[\nabla_{x^i} J(x)]\| \leqslant \beta(x) \tag{19}$$

where $\alpha(x)$ and $\beta(x)$ are finite scalar functions.

Using equation (19) with a stable sliding mode controller, the following equation can be obtained

$$\begin{aligned}\|s^i(t)\| &\leqslant \|s^i(0)\| = \|\dot{x}^i(0) \\ &\quad + \nabla_{x^i} J(x(0)) - \dot{x}_{\mathrm{SGC}_{\mathrm{command}}}(0)\| \leqslant \alpha(x(0)) \\ &\quad + \|\dot{x}^i(0) - \dot{x}_{\mathrm{SGC}_{\mathrm{command}}}(0)\| = K\end{aligned} \tag{20}$$

where K is a finite constant.

Substituting equations (19) and (20) in equation (18) yields

$$\begin{aligned}\left\| \frac{\mathrm{d}}{\mathrm{d}t}[\nabla_{x^i} J(x)] \right\| &\leqslant N\beta(x)[K + \alpha(x) + \|\dot{x}_{\mathrm{SGC}_{\mathrm{command}}}\|] \\ &\equiv \bar{J}_i(x)\end{aligned} \tag{21}$$

The following control law can be obtained by substituting equations (11) and (21) in equation (17).

$$u^i = -u_0^i(x)\,\mathrm{sign}\,(s^i) + [T_i(\psi)]^{-1} \ddot{x}_{\mathrm{SGC}_{\mathrm{command}}} \tag{22}$$

Substituting equation (22) in equation (17) yields

$$\begin{aligned}\dot{V}^i &= s^{i\mathrm{T}} \dot{s}^i = s^{i\mathrm{T}} \left\{ \mathbf{T}_i(\psi) \left[-u_0^i(x)\,\mathrm{sign}\,(s^i) - f_i \right] \right. \\ &\quad \left. + \frac{\mathrm{d}}{\mathrm{d}t}[\nabla_{x^i} J(x)] \right\} \\ &= -s^{i\mathrm{T}} \mathbf{T}_i(\psi) u_0^i(x)\,\mathrm{sign}\,(s^i) - s^{i\mathrm{T}} \mathbf{T}_i(\psi) f_i \\ &\quad + s^{i\mathrm{T}} \frac{\mathrm{d}}{\mathrm{d}t}[\nabla_{x^i} J(x)] \\ &\leqslant -\|s^{i\mathrm{T}}\| \|\mathbf{T}_i(\psi)\| u_0^i(x) + \|s^{i\mathrm{T}}\| \|\mathbf{T}_i(\psi)\| \|f_i\| \\ &\quad + \|s^{i\mathrm{T}}\| \left\| \frac{\mathrm{d}}{\mathrm{d}t}[\nabla_{x^i} J(x)] \right\| \\ &= -\|s^{i\mathrm{T}}\| u_0^i(x) + \|s^{i\mathrm{T}}\| \|f_i\| + \|s^{i\mathrm{T}}\| \left\| \frac{\mathrm{d}}{\mathrm{d}t}[\nabla_{x^i} J(x)] \right\| \\ &\leqslant -\|s^{i\mathrm{T}}\| u_0^i(x) + \|s^{i\mathrm{T}}\| \bar{f}_i + \|s^{i\mathrm{T}}\| \bar{J}_i(x) \\ &= -\|s^{i\mathrm{T}}\| [u_0^i(x) - \bar{f}_i - \bar{J}_i(x)]\end{aligned} \tag{23}$$

where $\|T_i(\psi)\| = 1$. The controller is chosen as

$$u_0^i(x) = \bar{f}_i + \bar{J}_i(x) + \varepsilon^i, \quad \varepsilon^i > 0 \tag{24}$$

Substituting equation (24) in equation (23) yields

$$\dot{V}^i \leqslant -\varepsilon^i \|s^i\| \tag{25}$$

Finally, the stability of the proposed control law is proved by the Lyapunov theory.

4 COLLISION AVOIDANCE

In this study, the swarm strategy is modified to have the ability of collision avoidance against the obstacles and pop-up threats. To do this, the potential function should be redefined.

4.1 Obstacle avoidance

Especially in an UAV formation flying, it is necessary to avoid the conflict with obstacles for completing the objectives of the mission. In the potential field method, the potential function term can be revised for collision avoidance without a big change in guidance law, that is

$$J(x) = J_{\text{swarm}}(x) + J_{\text{obstacle}}(x) \tag{26}$$

where $J_{\text{obstacle}}(x)$ should satisfy the following conditions, which are needed to fulfill the characteristics of the potential function to model the swarm behaviour.

Condition 1

$J_{\text{obstacle}}(x)$ includes the relative distance between the agent and the obstacle

$$J_{\text{obstacle}}(x) = \sum_{i=1}^{N} J_{\text{obstacle},\,i}(\rho^i), \quad \rho^i = \min \|x^i - q\| \tag{27}$$

where $q \in$ obstacle.

Condition 2

Repulsive potential affects in limited region

$$\|\nabla_{x^i} J_{\text{obstacle}}(\rho^i)\| = 0, \quad \rho^i > \rho_0 \tag{28}$$

where ρ_0 is the range of threat-effective area.

Condition 3

$J_{\text{obstacle}}(x)$ is in C^2 which satisfies equation (19)

$$\|J_{\text{obstacle},\,i}(\rho_1^i) - J_{\text{obstacle},\,i}(\rho_2^i)\| \leqslant L\|\rho_1^i - \rho_2^i\| \tag{29}$$

$$\|\nabla_{x^i} J_{\text{obstacle},\,i}(\rho_1^i) - \nabla_{x^i} J_{\text{obstacle},\,i}(\rho_2^i)\| \leqslant L\|\rho_1^i - \rho_2^i\|, \quad \rho_1^i, \rho_2^i \leqslant \rho_0 \tag{30}$$

where L is an inclination.

Consider the following potential function, which includes all obstacles to be avoided

$$J_{\text{obstacle}}(x) = \sum_{i=1}^{N} J_{\text{obstacle},\,i}(\rho^i) \tag{31}$$

$$\rho^i = \min \|x^i - q\| \tag{32}$$

Note that q is an obstacle, and ρ^i is a distance from ith UAV to the obstacle.

In this study, the following potential is defined

$$J_{\text{obstacle},\,i}(x^i) = \begin{cases} (1/2)\eta(1/\rho^i - 1/\rho_0)^2, & \rho(q) \leqslant \rho_0 \\ 0, & \rho(q) > \rho_0 \end{cases} \tag{33}$$

where ρ_0 is the distance under the influence of threat and $\eta > 0$. Note that equation (33) satisfies the threat conditions 1 to 3.

4.2 Pop-up threat avoidance

In case of the known obstacles, reference trajectory can be pre-generated considering the threat. Therefore, conflict with the known obstacles does not happen because threats are not located near the reference trajectory. For the unknown threats such as pop-up threat, however, there is a possibility that unknown

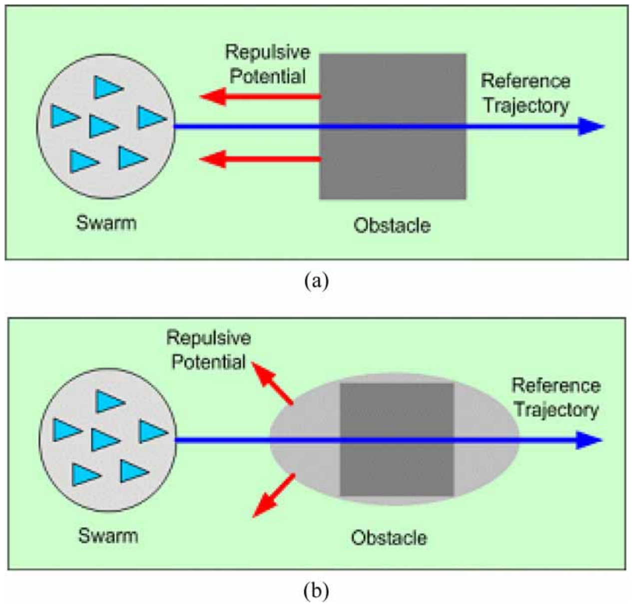

Fig. 1 Modified potential for pop-up threat avoidance: (a) local minima and (b) modified obstacle

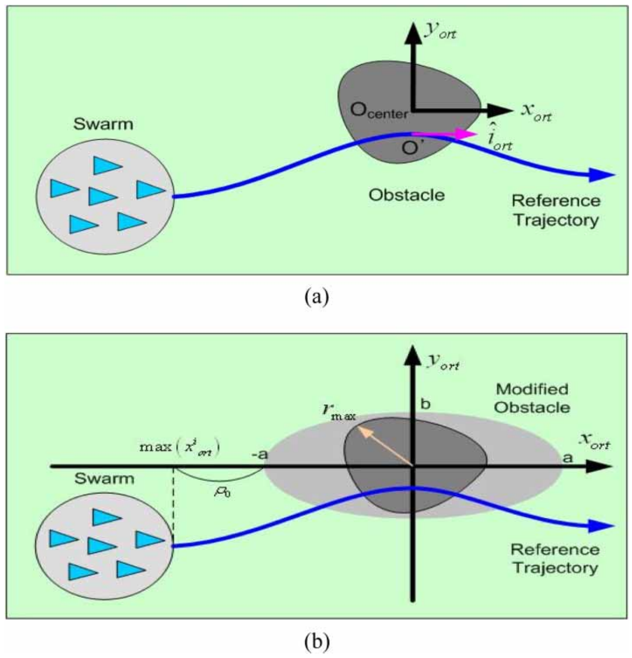

Fig. 2 Geometry of modified potential field: (a) obstacle coordinate and (b) modified obstacle potential field

threats are located on the reference path. With the benefits from the decentralized control, the pop-up threat near the reference trajectory can be avoided by adding the related potential function without modifying the reference path.

For the threats appearing on the trajectory as shown in Fig. 1(a), a local minima problem can be occurred due to the conflict of the velocity command to follow the reference trajectory ($\dot{x}_{\mathrm{SGC}_{\mathrm{command}}}$) and one of the repulsive potential ($-\nabla_{x^i} J_{\mathrm{obstacle}}(x)$). In case that the obstacle has a flat surface or a tangential point of a circle, the obstacle force counterbalances the force generated for reference tracking, and it may cause the local minima problem. In order to overcome this problem, the obstacle potential field is modified as shown in Fig. 1(b). When the threats are on the reference trajectory, the problem is solved by modifying the threat as an oval shape whose long-side direction is the same as the reference path. Modified oval shape obstacle can reflect the force in different directions. By doing this, the modified potential field brings an advantage of quick launch for evasive action as well as not having local minima.

Figure 2 shows how the modified obstacle potential field is designed when the UAVs detect pop-up threats along the path. A new coordinate, which includes the obstacle coordinate and reference trajectory coordinate, is defined. The X-axis is parallel with the tangential vector ($\hat{\boldsymbol{i}}$) of the reference trajectory and its origin is at the obstacle centre (O_{centre}). Positions of each agent and obstacle centre are expressed as

$$(x_{\mathrm{ort}}, y_{\mathrm{ort}}) = x_{\mathrm{ort}}\,\hat{\boldsymbol{i}} + y_{\mathrm{ort}}\,\hat{\boldsymbol{j}}; \quad O_{\mathrm{centre}} = (0, 0)_{\mathrm{ort}} \tag{34}$$

where $\hat{\boldsymbol{i}}, \hat{\boldsymbol{j}}$ are the unit direction vectors, and subscript ort the obstacle and reference trajectory coordinate.

In the ort-frame, let us define the modified obstacle as an oval shape, which includes the original obstacle as

$$\mathrm{MO} = \left[(x_{\mathrm{ort}}, y_{\mathrm{ort}}) \left| \frac{x_{\mathrm{ort}}^2}{a^2} + \frac{y_{\mathrm{ort}}^2}{b^2} \leqslant 1 \right. \right] \tag{35}$$

where a and b satisfy the following conditions

$$\begin{aligned} a &= \max[r_{\max}, -\max(x_{\mathrm{ort}}^i) - \rho_0] \\ b &= r_{\max} \end{aligned} \tag{36}$$

where $r_{\max} = \max(\|O - O_{\mathrm{centre}}\| | O \in \mathrm{obstacle})$ and ρ_0 is the distance under the effect of threat.

5 NUMERICAL SIMULATIONS

5.1 Simulation result for swarm without collision

The system architecture of the proposed decentralized swarm control is illustrated in Fig. 3. Simulation was performed with the parameters $c_1 = 0.01$, $c_2 = 20$, $c_3 = 10\,000$ and the distance between UAVs is set as $\delta_{ij} = 273$ ft. As shown in Fig. 4(a), all the agents converge to the centre without any collision to shape the formation. This shows that the proposed potential function, equation (6), guarantees a swarm aggregation. According to the characteristics of the potential function, the swarm shape and size can be changed by controlling the parameters c_i and δ_{ij} in equation (7). Consider the case of six agents in the formation of a triangular geometry. Setting up the suitable reference distance as

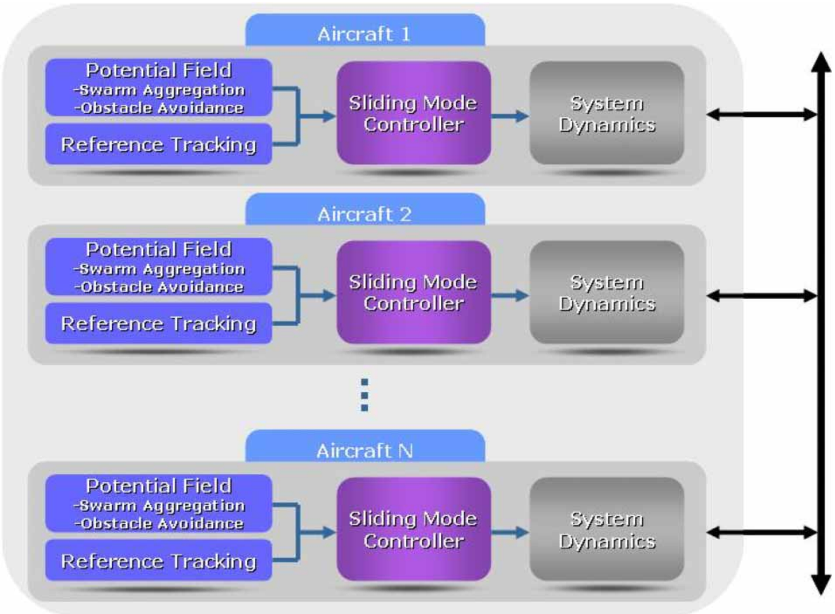

Fig. 3 System architecture

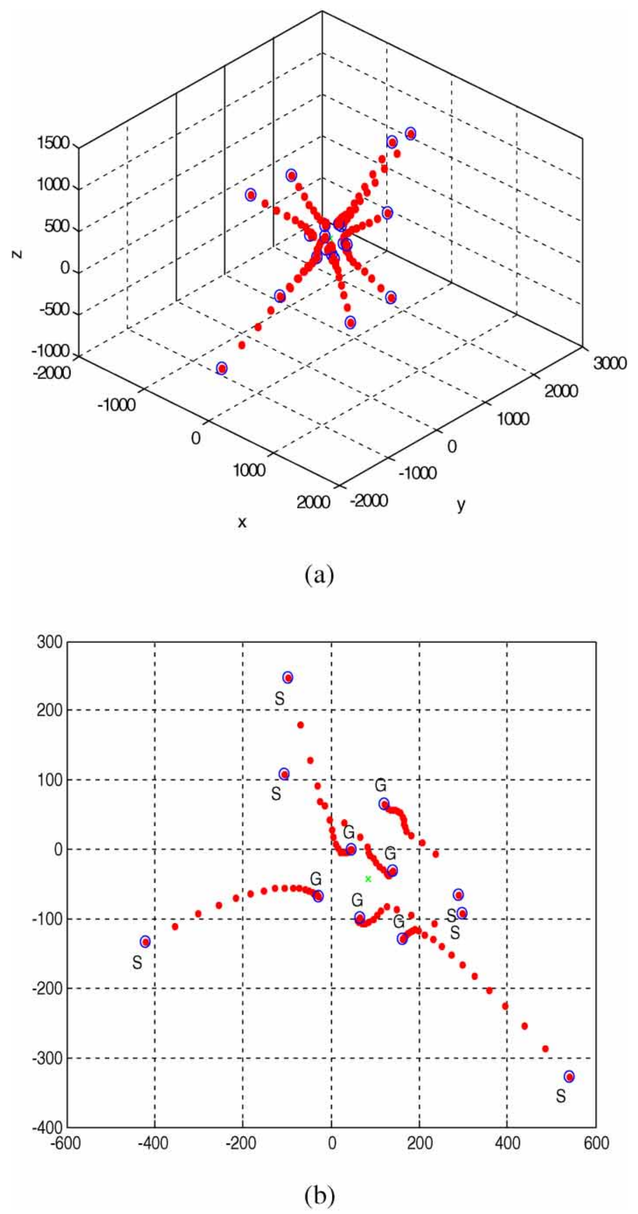

Fig. 4 Swarming behaviour and formation control: (a) swarming behaviour and (b) formation control

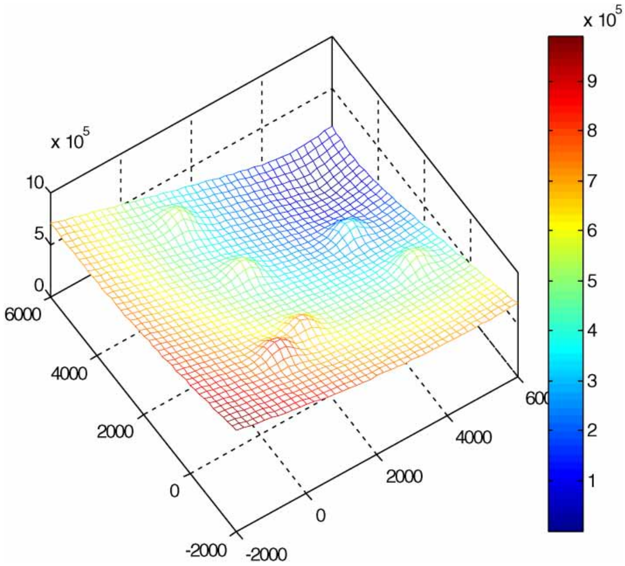

Fig. 5 Potential field

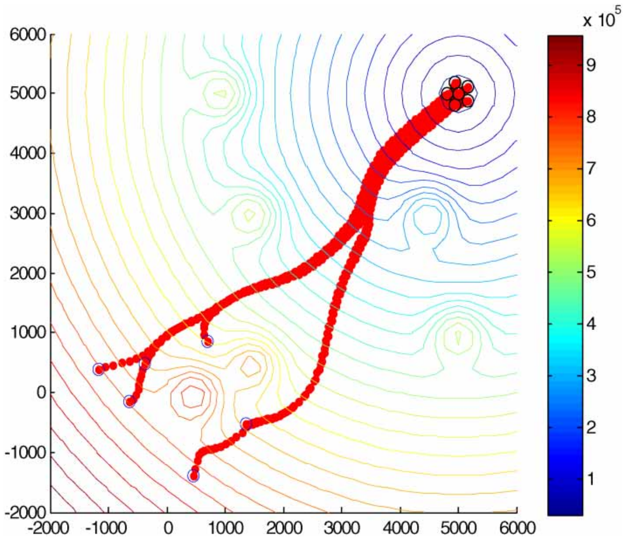

Fig. 6 Foraging swarm

$\delta_{ij} \in [100\ \ 100\sqrt{3}\ \ 200]$ results in a geometry as shown in Fig. 4(b) in which the UAVs converge to the designed formation shape without any conflict. The edged circle denotes the starting position (S) and the goal position (G) of each agent, and therefore individuals leave from point S and arrive at G. The trajectories of each agent are expressed as dots in Fig. 4.

5.2 Simulation result for the case of various threats

Consider mission environments including known obstacles and threats. Figure 5 shows the potential field considering the goal position and threats. As shown in Fig. 6, the proposed method makes the UAVs move to the desired goal without passing through the threat area. In simulations, the distance between UAVs is set as $\delta_{ij} = 100$ ft.

Simulations are also performed to validate the performance of tracking the reference path while keeping swarm geometry. Voronoi diagram and A* algorithm [**9**, **10**] are used to generate the reference trajectory for a problem with obstacles. To avoid collision with obstacles, all the obstacles are included in the potential function. System uncertainty is set $f_i = 0.1 \times \sin(0.2t)$, and velocity is bounded as $100 \leqslant V_i \leqslant 300$. Control input limitations are also considered: $\|u_1^i\| \leqslant 1.5G$ and $\|u_2^i\| \leqslant 3G$. Figure 7 shows the simulation result of reference tracking using SGC control and potential field

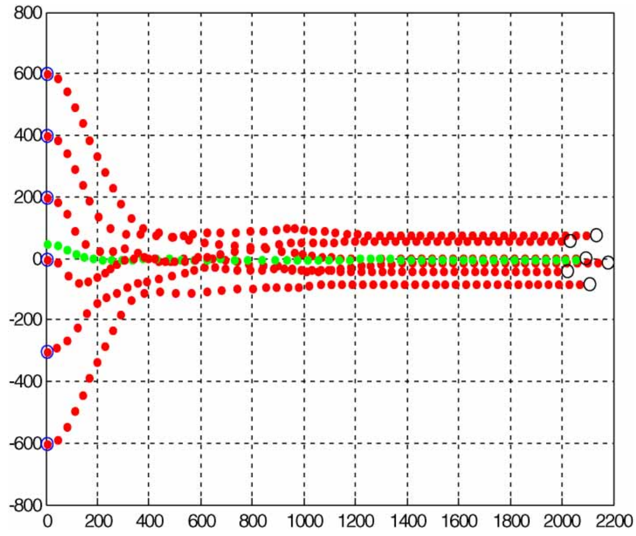

Fig. 7 Reference tracking using SGC control

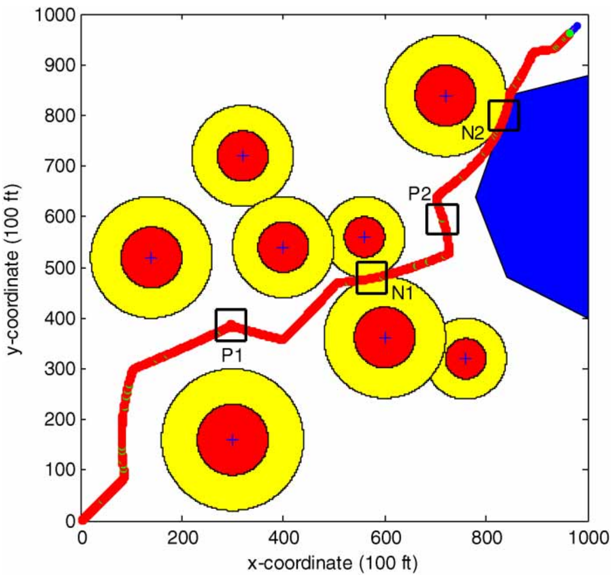

Fig. 8 Reference tracking with pop-up threat: narrow districts, N1, N2; pop-up districts, P1, P2

method. It is found that the UAVs move toward the desired points without any conflict with each other.

Figure 8 shows the simulation result in the case of known obstacles and pop-up obstacles. The tactical field from reference [**17**] is adopted for a more reasonable simulation scenario in which the UAVs need to fly avoiding the threat area, such as, radars and air defense systems. Total size of the battlefield is $100\,000 \times 100\,000\,\text{ft}^2$. Large outer circles represent the dangerous area according to the specifications of the radars, the small inner circles are the critical area, and the polygon denotes no-fly zone. Voronoi diagram and A* algorithm are used to generate a reference trajectory for SGC. The waypoints are quite far from each other, and the impact angle guidance law [**18**] is used to generate a more accurate path.

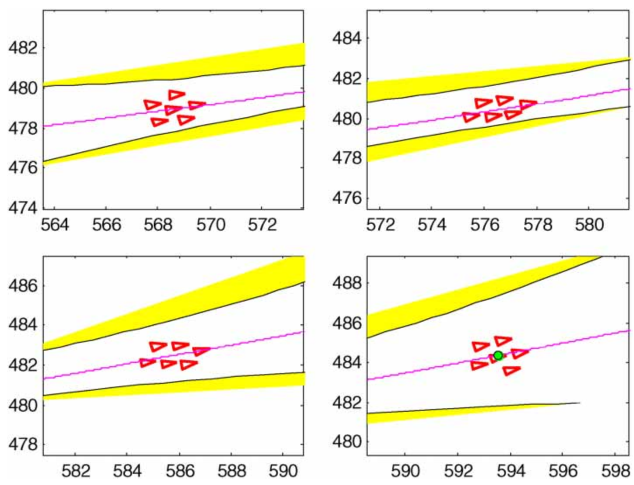

Fig. 9 Narrow district 1 (N1); unit 100 ft

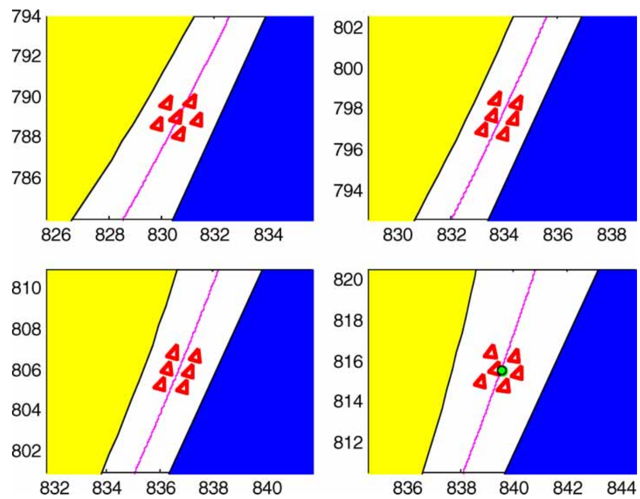

Fig. 10 Narrow district 2 (N2); unit 100 ft

In order to show how the UAV swarm passes the narrow area, which is smaller than the swarm size, the zoom-in figures of the narrow districts 1 and 2 in Fig. 8 are shown in Figs 9 and 10, respectively. The swarm geometry shrinks as the agents pass the narrow area and move freely to avoid collision. Moreover, to show how the UAV swarm deals with the pop-up threats, the zoom-in figures of pop-up districts (unknown threats) in Fig. 8 are shown in Figs 11 and 12. As shown in Figs 11 and 12, the pop-up threats are expressed as a circle and modified to an oval shape, and the UAVs are scattered when they meet the pop-up and get together after they escape from the pop-up threat area. Table 1 summarizes the minimum distance between UAVs, UAV and known obstacles, and UAV and pop-up threats. In summary, excellent swarm behaviours are observed

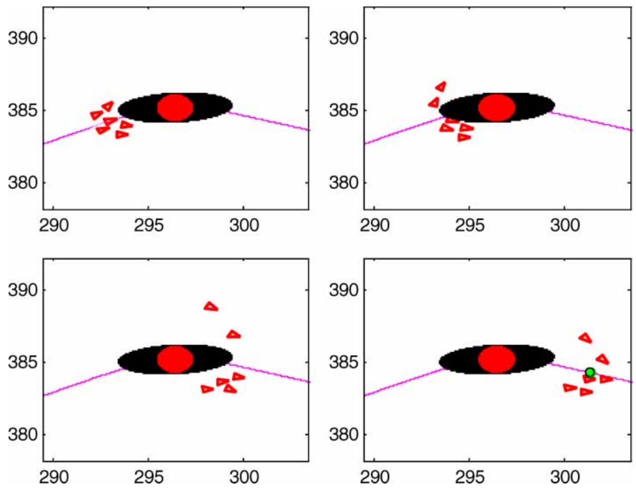

Fig. 11 Pop-up district 1 (P1); unit 100 ft

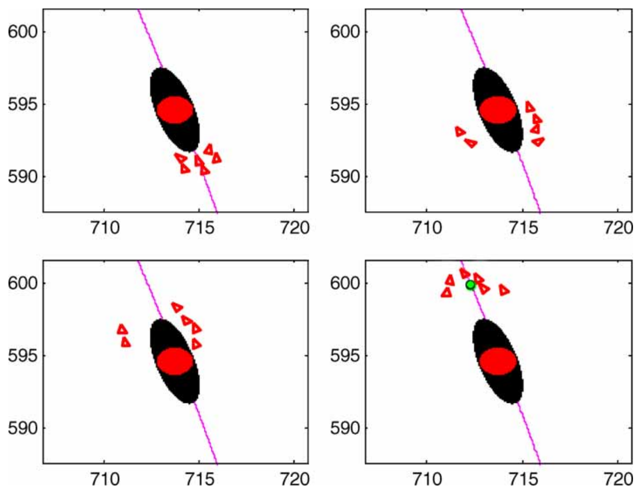

Fig. 12 Pop-up district 2 (P2); unit 100 ft

Table 1 Minimum distances

	Minimum distance between UAVs (ft)	Minimum distance between UAV and known obstacles (ft)	Minimum distance between UAV and pop-up threat (ft)
UAV 1	51.23	74.28	79.49
UAV 2	32.97	80.48	65.20
UAV 3	51.23	66.91	28.42
UAV 4	44.74	49.39	96.71
UAV 5	55.13	39.47	38.39
UAV 6	32.97	45.25	58.39

even when pop-up threats appear along the path. All agents do not collide with any obstacles and keep the geometrical shape while the SGC follows the desired trajectory.

6 CONCLUSION

In this paper, swarm aggregation using artificial potential function and SGC strategy is proposed. The decentralized swarm controller is utilized based on the sliding mode controller. Decentralized swarm guidance and control has an advantage of dealing with varying environments by simply adding a potential function. The potential functions can treat various swarm geometrical shape as well as the collision problem with obstacles and other agents. The proposed strategy can be used for the formation reconfiguration and relocation of UAVs, satellites, and mobile robots.

ACKNOWLEDGEMENT

This work was supported by the Korea Science and Engineering Foundation (KOSEF) grant funded by the Korean government (MOST) (no. R0A-2007-000-10017-0).

REFERENCES

1 **Park, C. S., Tahk, M. J.,** and **Bang, H. C.** Multiple aerial vehicle formation using swarm intelligence. In the AIAA Guidance, Navigation, and Control Conference, Austin, TX, USA, 2003, AIAA paper 2003-5729.

2 **Gazi, V.** and **Passino, K. M.** Biased stability analysis of swarms. *IEEE Trans. Autom. Control*, 2003, **48**(4), 692–697.

3 **Gazi, V.** Swarm aggregations using artificial potentials and sliding-mode control. *IEEE Trans. Robot.*, 2005, **21**(6), 1208–1214.

4 **Utkins, V. I., Drakunov, S. V., Hashimoto, H.,** and **Harashima, F.** Robot path obstacle avoidance control via sliding mode approach. In the IEEE/RSJ International Workshop Intelligence Robots System, Osaka, Japan, 1991, pp. 1287–1290.

5 **Guldner, J.** and **Utkin, V. I.** Sliding mode control for an obstacle avoidance strategy based on an harmonic potential field. In the IEEE Conference on Decision and Control, San Antonio, TX, 1993, pp. 424–429.

6 **Guldner, J.** and **Utkin, V. I.** Sliding mode control for gradient tracking and robot navigation using artificial potential fields. *IEEE Trans. Robot. Autom. Control*, 1995, **11**(2), 247–254.

7 **Gazi, V.** and **Ordonez, R.** Target tracking using artificial potentials and sliding mode control. In the American Control Conference, Boston, MA, 2004, pp. 5588–5593.

8 **Yao, J., Ordonez, R.,** and **Gazi, V.** Swarm tracking using artificial potentials and sliding mode control. *J. Dyn. Syst. Meas. Control*, 2007, **129**, 749–754.

9 **Krozel, J.** and **Andrisani, D.** Navigation path planning for autonomous aircraft: Voronoi diagram approach. *J. Guid. Control Dyn.*, 1990, **13**(6), 1152–1154.

10 **Hart, P. E., Nilsson, N. J.,** and **Raphael, B.** A formal basis for the heuristic determination of minimum

cost paths. *IEEE Trans. Syst. Sci. Cybernet.*, 1968, **4**(2), 100–107.

11 **Gazi, V.** and **Passino, K. M.** A class of attractions/repulsion functions for stable swarm aggregations. *Int. J. Control*, 2004, **77**(18), 1567–1579.

12 **Giulietti, F., Pollini, L.,** and **Innocenti, M.** Formation flight control: a behavioral approach. In the AIAA Guidance, Navigation, and Control Conference, Montreal, Canada, 2001, AIAA paper 2001-4239.

13 **Giulietti, F., Innocenti, M., Napolitano, M.,** and **Pollini, L.** Dynamic and control issues of formation flight. *Aerosp. Sci. Technol.*, 2005, **9**(1), 65–71.

14 **Wolfe, J. D., Chichka, D. F.,** and **Speyer, J. L.** Decentralized controllers for unmanned aerial vehicle formation flight. In the AIAA Guidance, Navigation, and Control Conference, San Diego, CA, USA, 1996, AIAA paper 1996-3833.

15 **Reynolds, C.** Flocks, herds, and schools: a distributed behavioral model. *SIGGRAPH Comput. Graph.*, 1987, **21**(4), 25–34.

16 **Khatib, O.** Real-time obstacle avoidance for manipulators and mobile robots. *Int. J. Robot. Res.*, 1986, **5**(1), 90–98.

17 **Eun, Y. J.** and **Bang, H. C.** Cooperative control of multiple unmanned aerial vehicles using the potential field theory. *J. Aircr.*, 2006, **43**(6), 1805–1814.

18 **Jung, B. K.** and **Kim, Y.** Guidance laws for anti-ship missiles using impact angle and impact time. In the AIAA Guidance, Navigation, and Control Conference, Keystone, Colorado, USA, 2006, AIAA paper 2006-6432.